# Hyperbolic Ricci Flow and Its Application in Studying Lateral Ventricle Morphometry

Jie Shi[1], Paul M. Thompson[2], and Yalin Wang[1]

[1] School of Computing, Informatics and Decision Systems Engineering, Arizona State University, Tempe, AZ 85281, USA
[2] Laboratory of Neuro Imaging, Department of Neurology, UCLA School of Medicine, Los Angeles, CA 90095, USA
{jie.shi,ylwang}@asu.edu, thompson@loni.ucla.edu

**Abstract.** Here we propose a novel method to compute surface hyperbolic parameterization for studying brain morphology with the Ricci flow method. Two surfaces are conformally equivalent if there exists a bijective angle-preserving map between them. The Teichmüller space for surfaces with the same topology is a finite-dimensional manifold, where each point represents a conformal equivalence class, and the conformal map is homotopic to the identity map. A shape index can be defined based on Teichmüller space coordinates, and this shape index is intrinsic and invariant under scaling, translation, rotation, general isometric deformation, and conformal deformation. Using the Ricci flow method, we can conformally map a surface with a negative Euler number to the Poincaré disk and the Teichmüller space coordinates can be computed by geodesic lengths under hyperbolic metric. For lateral ventricular surface registration, we further convert the parameterization to the Klein model where a convex polygon is guaranteed for a multiply connected surface. With the Klein model, diffeomorphisms between lateral ventricular surfaces can be computed with some well known surface registration methods. Compared with prior work, the parameterization does not have any singularities and the intrinsic parameterizations help shape indexing and surface registration. Our preliminary experimental results showed its great promise for analyzing anatomical surface morphology.

## 1 Introduction

Shape analysis is a key research topic in anatomical modeling and statistical comparisons of anatomy. In studies that analyze brain morphology, many shape analysis methods have been proposed, such as spherical harmonic analysis (SPHARM) [1, 2], medial representations (M-reps) [3], and minimum description length approaches [4], etc.; these methods may also be applied to analyze shape changes or abnormalities in subcortical brain structures. Recent work has also taken a population based approach by analyzing surface changes using pointwise displacements of surface meshes, local deformation tensors, or surface expansion factors [5, 6]. Even so, a stable method to compute transformation-invariant shape descriptors and diffeomorphisms between topology complicated surfaces would be highly advantageous in this research field. Here we propose a

P.-T. Yap et al. (Eds.): MBIA 2012, LNCS 7509, pp. 61–76, 2012.

novel and intrinsic method to compute hyperbolic conformal parameterization of surfaces with negative Euler numbers with hyperbolic Ricci flow method. We use lateral ventricular morphometry as an example to demonstrate our algorithm in a dataset from our prior research [7, 8].

All oriented surfaces have conformal structures. The conformal structure is, in some respects, more flexible than the Riemannian metric but places more restrictions on the surface morphology than the topological structure. According to Klein's Erlangen program, different geometries study the invariants under different transformation groups. Conformal geometry corresponds to the angle-preserving transformations. If there exists a conformal map between two surfaces, they are conformally equivalent. All surfaces may be classified by the conformal equivalence relation. For surfaces with the same topology, the Teichmüller space is a natural finite-dimensional manifold, where each point represents a conformal equivalence class and the distance between two shapes can be accurately measured. A shape index can be defined based on Teichmüller space coordinates. This shape index is intrinsic and invariant under conformal transformations, rigid motions and scaling. It is simple to compute; no surface registration is needed. It is very general; it can handle all arbitrary topology surfaces with negative Euler numbers.

In this work, only genus-zero surfaces with three boundaries are considered. With the discrete version of the surface Ricci flow method (also called the discrete Ricci flow), we conformally projected the surfaces to the hyperbolic plane and isometrically embedded them in the Poincaré disk. The proposed Teichmüller space coordinates are the lengths of a special set of geodesics under this special hyperbolic metric. Next, we computed the Klein model of the hyperbolic parameterization. The obtained convex polygon provides a stable parameter domain for surface registration. Compared with prior work [8], the new registration method relies on surface intrinsic features and does not have any singularities. It provides a promising way to analyze complex ventricular morphometry using MR images.

We tested our algorithm on cortical and lateral ventricular surfaces extracted from 3D anatomical brain MRI scans. The proposed algorithm can map the profile of differences in surface morphology between healthy controls and subjects with HIV/AIDS. Finally, we applied our algorithm to compare the intrinsic features of two ventricular surfaces with strong shape difference to demonstrate the feasibility of applying the new method for surface registration.

### 1.1 Related Work

In the computational analysis of brain anatomy, volumetric measures of structures identified on 3D MRI have been used to study group differences in brain structure and also to predict diagnosis [9, 10, 11]. However, early research [12, 13, 14, 15] has demonstrated that surface-based approaches may offer advantages as a method to register brain images. To register brain surfaces, a common approach is to compute a range of intermediate mappings to some canonical parameter space [6, 12, 13, 16, 17, 18]. A flow, computed in the parameter space

of the two surfaces, then induces a correspondence field in 3D [19]. This flow can be constrained by anatomical landmark points or curves [20, 21, 22, 23, 24], by subregions of interest [25], by using currents to represent anatomical variation [26, 27], or by metamorphoses [28]. Various ways also exist for optimizing surface registrations [29, 30, 31, 32].

Recent work has also used shape-based features (reviewed in [33]). Many surface based statistics were studied for evaluating disease burden, progression and response to interventions, including m-rep [3], SPHARM [2], principal geodesic analysis [34], random orbit model [35], deformation-based morphometry (DBM) [36, 37], tensor-based morphometry (TBM) [1, 38], Teichmüller shape space [39, 40], Laplace-Beltrami eigen function [41], $q$-maps [42], and optimal mass transportation [29], etc.

Some work has focused on conformal parameterization of brain surfaces. There are mainly five categories of methods for brain surface study: quasiconformal mapping with circle packing [43], Cauchy-Riemann equation [44, 45, 46], harmonic maps [47], holomorphic differentials [48], and Ricci/Yamabe flow method [49, 50]. Among all these algorithms, only the holomorphic differentials [48, 51], Ricci flow methods [49, 50] and circle packing method [43] work on high genus surfaces while circle packing method can only generate quasi-conformal mapping (see a discussion in [50]).

With the Ricci flow method, Wang et al. [50] solved the Yamabe equation and conformally mapped the cortical surface of the brain to a Euclidean multi-hole punctured disk. Gu et al. applied the surface Ricci flow method to study general 3D shape matching and registration. The hyperbolic Ricci flow has also been applied to study 3D face matching. Recently, Jin et al. [39] and Zeng et al. [52] introduced the Teichmüller shape space to index and compare general surfaces with various topologies, geometries and resolutions.

## 2 Theoretical Background and Definitions

This section briefly introduces the theoretic background and definitions necessary for the current work.

*Conformal Deformation.* Suppose $S$ is a surface embedded in $\mathbb{R}^3$ with a Riemannian metric $\mathbf{g}$ induced from the Euclidean metric. Let $u : S \to \mathbb{R}$ be a scalar function on $S$. It can be verified that $\tilde{\mathbf{g}} = e^{2u}\mathbf{g}$ is also a Riemannian metric on $S$ and angles measured by $\mathbf{g}$ are equal to those measured by $\tilde{\mathbf{g}}$. Thus, $\tilde{\mathbf{g}}$ is called a *conformal deformation* of $\mathbf{g}$.

The Gaussian curvature of the surface will also be changed accordingly and become $\tilde{K} = e^{-2u}(-\Delta_{\mathbf{g}} u + K)$, where $\Delta_{\mathbf{g}}$ is the Laplacian-Beltrami operator under the original metric $\mathbf{g}$. The geodesic curvature will become $\tilde{k_g} = e^{-u}(\partial_{\mathbf{r}} u + k_g)$, where $\mathbf{r}$ is the tangent vector orthogonal to the boundary. According to Gauss-Bonnet theorem, the total curvature is $2\pi\chi(S)$, where $\chi(S)$ is the Euler characteristic number of $S$.

*Uniformization Theorem.* [53]. Given a surface $S$ with a Riemannian metric $\mathbf{g}$, there exist an infinite number of metrics conformal to $\mathbf{g}$. The uniformization theorem states that, among all conformal metrics, there exists a unique representative, which induces constant Gaussian curvature everywhere. Moreover, the constant will be one of $\{+1, 0, -1\}$. Therefore, we can embed the universal covering space of any closed surface using its uniformization metric onto one of the three canonical surfaces: the *sphere* $\mathbb{S}^2$ for genus-0 surfaces with positive Euler numbers, the *plane* $\mathbb{E}^2$ for genus-1 surfaces with zero Euler number, and the *hyperbolic space* $\mathbb{H}^2$ for high genus surfaces with negative Euler numbers. Accordingly, we can say that surfaces with positive Euler number admit spherical geometry; surfaces with zero Euler number admit Euclidean geometry; and surfaces with negative Euler number admit hyperbolic geometry.

*Poincaré Disk Model.* In this work, we specify the background geometry of all surfaces as the hyperbolic space $\mathbb{H}^2$. The hyperbolic space cannot be realized in $\mathbb{R}^3$, thus we use the Poincaré disk to model it. The Poincaré disk is the unit disk $|z| < 1$ in the complex plane with the metric $ds^2 = \frac{4dzd\bar{z}}{(1-z\bar{z})^2}$. The rigid motion in hyperbolic space is the Möbius transformation $z \to e^{i\theta}\frac{z-z_0}{1-\bar{z}_0 z}$, where $\theta$ and $z_0$ are parameters. The geodesics on the Poincaré disk are arcs of Euclidean circles, which intersect the boundary of the the unit circle at right angles.

*Hyperbolic Ricci Flow.* In this work we use the surface Ricci flow method to conformally project the surfaces to the hyperbolic plane and isometrically embed them in the Poincaré disk. We call this method hyperbolic Ricci flow.

Let $S$ be a smooth surface with a Riemannian metric $\mathbf{g} = (g_{ij})$. The Ricci flow deforms the metric $\mathbf{g}(t)$ according to the Gaussian curvature $K(t)$,

$$\frac{dg_{ij}(t)}{dt} = -2K(t)g_{ij}(t),$$

where $t$ is the time parameter. With $\mathbf{g}(t) = e^{2u(t)}\mathbf{g}(0)$, the Ricci flow can be simplified as

$$\frac{du(t)}{dt} = -2K(t).$$

*Fuchsian Transformation.* Suppose $S$ is a surface with a negative Euler number and its hyperbolic uniformization metric is $\tilde{\mathbf{g}}$. Then its universal covering space $(\tilde{S}, \tilde{\mathbf{g}})$ can be isometrically embedded in $\mathbb{H}^2$. Any deck transformation of $\tilde{S}$, which is a transformation from one universal covering space to another and keeps projection invariant, is a Möbius transformation and called a *Fuchsian transformation*. Let $\phi$ be a Fuchsian transformation, let $z \in \mathbb{H}^2$, the *attractor* and *repulser* of $\phi$ are $\lim_{n\to\infty} \phi^n(z)$ and $\lim_{n\to\infty} \phi^{-n}(z)$, respectively. The *axis* of $\phi$ is the unique geodesic through its attractor and repulser. The deck transformation group is called the *Fuchsian group* of $S$.

Fig. 1 (a) and (b) illustrate some basic concepts in hyperbolic geometry. (a) shows a saddle-shape plane which has constant negative Gaussian curvatures. (b) shows Escher's famous prints *Circle Limit III* [54], where the white lines are close to geodesics, i.e. hypercycles, on the Poincaré disk.

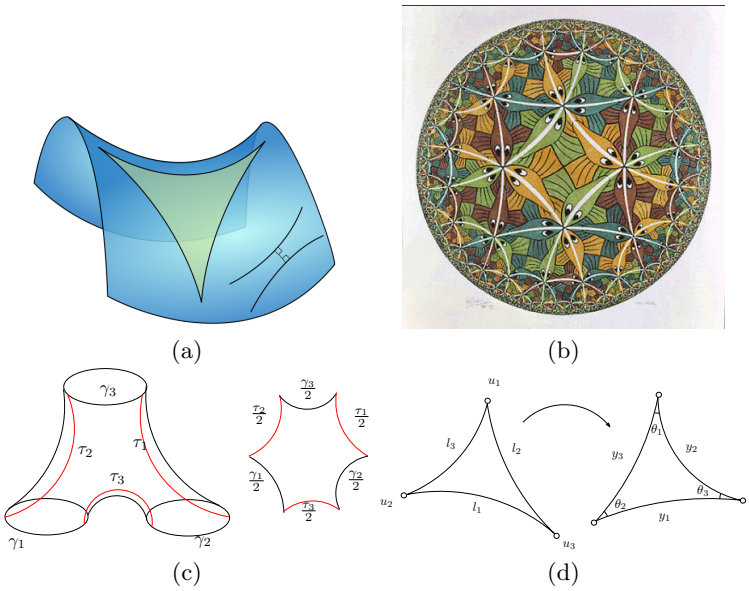


**Fig. 1.** Some simple illustrations of hyperbolic geometry. (a) a saddle-shape plane with constant negative Gaussian curvatures. (b) Escher's prints Circle Limit III [54]. (c) a pair of hyperbolic pants. (d) conformal transformation between two hyperbolic triangles.

*Teichmüller Space.* Let $(S_1, \mathbf{g}_1)$ and $(S_2, \mathbf{g}_2)$ be two metric surfaces, and let $f : S_1 \to S_2$ be a differential map between them. If the pull-back metric induced by $f$ satisfies the following condition:

$$\mathbf{g}_1 = e^{2\lambda} f^* \mathbf{g}_2,$$

then we say the map is *conformal*. Two metric surfaces are conformally equivalent, if there exists an invertible conformal map between them. All surfaces may be classified using this conformal equivalence relation.

All conformal equivalence classes of surface with a fixed topology form a finite-dimensional manifold, the so-called Teichmüller space. Teichmüller space is a shape space, where a point represents a class of surfaces, and a curve in Teichmüller space represents a deformation process from one shape to the other. The coordinates of the surface in Teichmüller space can be explicitly computed. The Riemannian metric of The Teichmüller space is also well-defined.

As an example, Fig. 1 (c) shows a genus-zero surface with three boundaries $\partial S = \{\gamma_1, \gamma_2, \gamma_3\}$, which is also called *topological pants*. If the length of boundary $\gamma_i$ is $l_i$ under the hyperbolic uniformization metric, then $(l_1, l_2, l_3)$ are the Teichmüller coordinates of $S$ in the Teichmüller space of all conformal classes of a pair of pants. Namely, if two surfaces share the same Teichmüller coordinates, they can be conformally mapped to each other. In this work, only surfaces with the pants topology are considered.

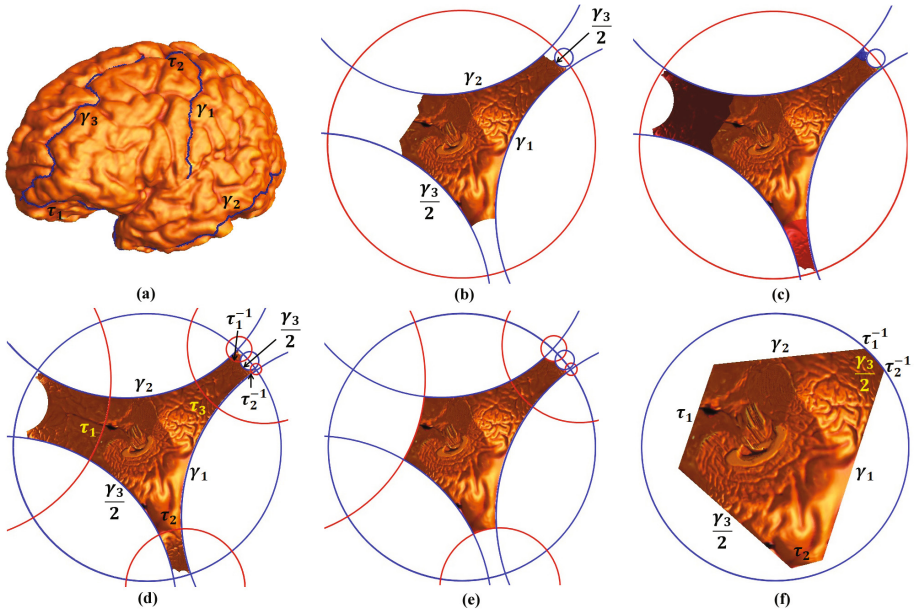


**Fig. 2.** Illustration of computation of hyperbolic conformal parameterization of a left cortical surface with Ricci flow method.

*Klein Model.* In additional to Poincaré model, there also exist other models of hyperbolic space. Another commonly used one is the *Klein model* [55]. The Klein model is also the unit disk, where all geodesics are straight Euclidean lines. The obtained convex polygon simplifies the computation and provides a convex domain for further surface registration methods. The conversion from the Poincaré disk to the Klein model is

$$z \to \frac{2z}{1+\bar{z}z} \tag{1}$$

The Poincaré model is conformal, whereas the Klein model is not. In our Poincaré model, we compute the shortest lines between two hyperbolic lines. The lines are unique because they are the geodesics on the hyperbolic space. So the converted Klein model is convex and uniquely determined by the intrinsic surface shape. It provides a practical and efficient domain for us to compute diffeomorphisms between topology complicated surfaces.

## 3 Computational Algorithms

This section details the algorithms for computing the hyperbolic metric, the Teichmüller coordinates and surface diffeomorphisms via the hyperbolic parameterization.

### 3.1 Computing Hyperbolic Metric of a Surface with the Ricci Flow Method

In practice, most surfaces are approximated by discrete triangular meshes. Let $M$ be a two-dimensional simplicial complex. We denote the set of vertices, edges and faces by $V, E, F$, respectively. We call the $ith$ vertex $v_i$; edge $[v_i, v_j]$ runs from $v_i$ to $v_j$; and the face $[v_i, v_j, v_k]$ has its vertices sorted counter-clockwise. In this work, we assume all faces are hyperbolic triangles. Fig. 1 (d) illustrates the conformal transformation between a pair of hyperbolic triangles and their associated edge lengths $l_i, y_i$, corner angles $\theta_i$ and conformal factor $u_i$.

A *discrete metric* is a function $l : E \to \mathbb{R}^+$, such that triangle inequality holds on every face, which represents the edge lengths. The *discrete curvature* $K : V \to \mathbb{R}$ is defined as the angle deficit, i.e., $2\pi$ minus the surrounding corner angles for an interior vertex, and $\pi$ minus the surrounding corner angles for a boundary vertex.

Suppose the mesh is embedded in $\mathbb{R}^3$, so it has the induced Euclidean metric. We use $l^0_{ij}$ to denote the initial induced Euclidean metric on edge $[v_i, v_j]$.

Let $u : V \to \mathbb{R}$ be the *discrete conformal factor*. The discrete conformal metric deformation is defined as

$$\sinh(\frac{y_k}{2}) = e^{u_i} \sinh(\frac{l_k}{2}) e^{u_j}. \tag{2}$$

The *discrete Ricci flow* is defined as

$$\frac{du_i}{dt} = -K_i, \tag{3}$$

where $K_i$ is the curvature at the vertex $v_i$.

Let $\mathbf{u} = (u_1, u_2, \cdots, u_n)$ be the conformal factor vector, where $n$ is the number of vertices, and $\mathbf{u_0} = (0, 0, \cdots, 0)$. Then the *discrete hyperbolic Yamabe energy* is defined as

$$E(\mathbf{u}) = \int_{\mathbf{u_0}}^{\mathbf{u}} \sum_{i=1}^{n} K_i du_i. \tag{4}$$

The differential 1-form $\omega = \sum_{i=1}^{n} K_i du_i$ is closed. We use $c_k$ to denote $\cosh(y_k)$. By direct computation, it can be shown that on each triangle,

$$\frac{\partial \theta_i}{\partial u_j} = A \frac{c_i + c_j - c_k - 1}{c_k + 1},$$

where

$$A = \frac{1}{\sin(\theta_k) \sinh(y_i) \sinh(y_j)},$$

which is symmetric in $i, j$, so $\frac{\partial \theta_i}{\partial u_j} = \frac{\partial \theta_j}{\partial u_i}$. It is easy to see that $\frac{\partial K_i}{\partial u_j} = \frac{\partial K_j}{\partial u_i}$, which implies $d\omega = 0$. The discrete hyperbolic Yamabe energy is convex. The unique global minimum corresponds to the hyperbolic metric with zero vertex curvatures.

This requires us to compute the Hessian matrix of the energy. The explicit form is given as follows:

$$\frac{\partial \theta_i}{\partial u_i} = -A\frac{2c_ic_jc_k - c_j^2 - c_k^2 + c_ic_j + c_ic_k - c_j - c_k}{(c_j+1)(c_k+1)}$$

The Hessian matrix $(h_{ij})$ of the hyperbolic Yamabe energy can be computed explicitly. Let $[v_i, v_j]$ be an edge, connecting two faces $[v_i, v_j, v_k]$ and $[v_j, v_i, v_l]$. Then the edge weight is defined as

$$h_{ij} = \frac{\partial \theta_i^{jk}}{\partial u_j} + \frac{\partial \theta_i^{lj}}{\partial u_j}.$$

also for

$$h_{ii} = \sum_{j,k} \frac{\partial \theta_i^{jk}}{\partial u_i},$$

where the summation goes through all faces surrounding $v_i$, $[v_i, v_j, v_k]$.

The discrete hyperbolic energy can be directly optimized using Newton's method. Because the energy is convex, the optimization process is stable.

Given the mesh $M$, a conformal factor vector $\mathbf{u}$ is *admissible* if the deformed metric satisfies the triangle inequality on each face. The space of all admissible conformal factors is not convex. In practice, the step length in Newton's method needs to be adjusted. Once the triangle inequality no longer holds on a face, then an edge swap needs to be performed. The target hyperbolic metric computed by the Ricci flow method can be used to isometrically embed the surface in the Poincaré disk.

Fig. 2 (a) and (b) illustrate the hyperbolic Ricci flow method. (a) shows the initial cortical surface with three boundaries $\gamma_1, \gamma_2, \gamma_3$, which were cut along specific anatomical landmarks. The curves $\tau_1$ and $\tau_2$ are the shortest paths connecting $\gamma_2$ and $\gamma_3$, $\gamma_1$ and $\gamma_3$, respectively. We cut the surface open along $\tau_1$ and $\tau_2$ to obtain a simply connected surface $\tilde{S}$. By running the hyperbolic Ricci flow, the hyperbolic metric is obtained. With the metric, $\tilde{S}$ can be isometrically embedded onto the Poincaré disk as shown in (b). The boundaries of the original surface, $\gamma_1, \gamma_2, \gamma_3$, map to geodesics.

### 3.2 Computing the Teichmüller coordinates

In order to compute the Teichmüller coordinates of a surface with the hyperbolic metric obtained with the Ricci flow method in Sec. 3.1, we need to compute the Fuchsian group generators of the surface. As illustrated in Fig. 2, the Möbius transformations $\phi_1$ that transforms $\tau_1$ to $\tau_1^{-1}$ and $\phi_2$ that transforms $\tau_2$ to $\tau_2^{-1}$ form the generators of the Fuchsian group of the surface in Fig. 2 (a). In Fig. 2 (c), the embedding of $\tilde{S}$ is transformed by a Fuchsian transformation. Each color represents a copy of $\tilde{S}$. Frame (d) shows the computation of $\tau_i$'s, which are the shortest geodesics connecting the geodesic boundaries $\gamma_j$ and $\gamma_k$.

The final result is shown in Fig. 2 (e). The lengths of $\gamma_1, \gamma_2, \gamma_3$ in the hyperbolic space are the Teichmüller coordinates of $S$.

### 3.3 Surface Registration with the Klein Model

After we compute the Poincaré model, we can transform the hyperbolic polygon from the Poincaré model to the Klein model with Eqn. 1. The result is shown in Figure 2 (f). The polygon becomes a Euclidean convex polygon. We can apply either constrained harmonic map [8] or surface fluid registration method [56] to compute surface registration. Both methods will generate differeomorphisms since harmonic maps between convex planar polygons are diffeomorphisms and the surface fluid registration method also guarantees diffeomorphisms. The registered ventricular surfaces may provide a rigorous theoretic foundation to build ventricular atlas with population-based brain imaging approaches [5, 6].

## 4 Experimental Results

The lateral ventricles - fluid-filled structures deep in the brain - are often enlarged in disease and can provide sensitive measures of disease progression [7, 57, 58, 59]. Ventricular changes reflect atrophy in surrounding structures, and ventricular measures and surface-based maps can provide sensitive assessments of tissue reduction that correlate with cognitive deterioration in illnesses. However, the concave shape, complex branching topology and narrowness of the inferior and posterior horns have made automatic analyses more difficult.

With the hyperbolic Ricci flow method, we proposed two methods to analyze lateral ventricular morphometry: (1) to quantify lateral ventricular surface morphometry with the Teichmüller shape space coordinates; (2) to register lateral ventricular surfaces via the Klein model. In this section, we report our preliminary results on a HIV/AIDS dataset used in our prior research [7, 8].

### 4.1 Quantifying Lateral Ventricular Surface Morphology with the Teichmüller Shape Space Coordinates

To model the lateral ventricular surface, we automatically locate and introduce three cuts on each ventricle. The cuts are motivated by examining the topology of the lateral ventricles, in which several horns are joined together at the ventricular "atrium" or "trigone". We call this topological model, creating a set of connected surfaces, a *topology optimization* operation. After modeling the topology in this way, a lateral ventricular surface, in each hemisphere, becomes an open boundary surface with 3 boundaries, a topological pant surface.

After the topology optimization, a ventricular surface is topologically equivalent to a topological pant surface. We can then compute its Teichmüller space coordinate. Figure 3 illustrates how to compute Teichmüller space coordinates for a lateral ventricle. In the figure, $\gamma_1$, $\gamma_2$, and $\gamma_3$ are labeled boundaries and $\tau_1$ and $\tau_2$ are the shortest geodesics between boundaries. Figure 3 (d) illustrates the surface with the hyperbolic metric that is isometrically flattened onto the Poincaré disk. When we make the topological change, we make sure each new boundary has the same Euclidean length across different surface. As a result,

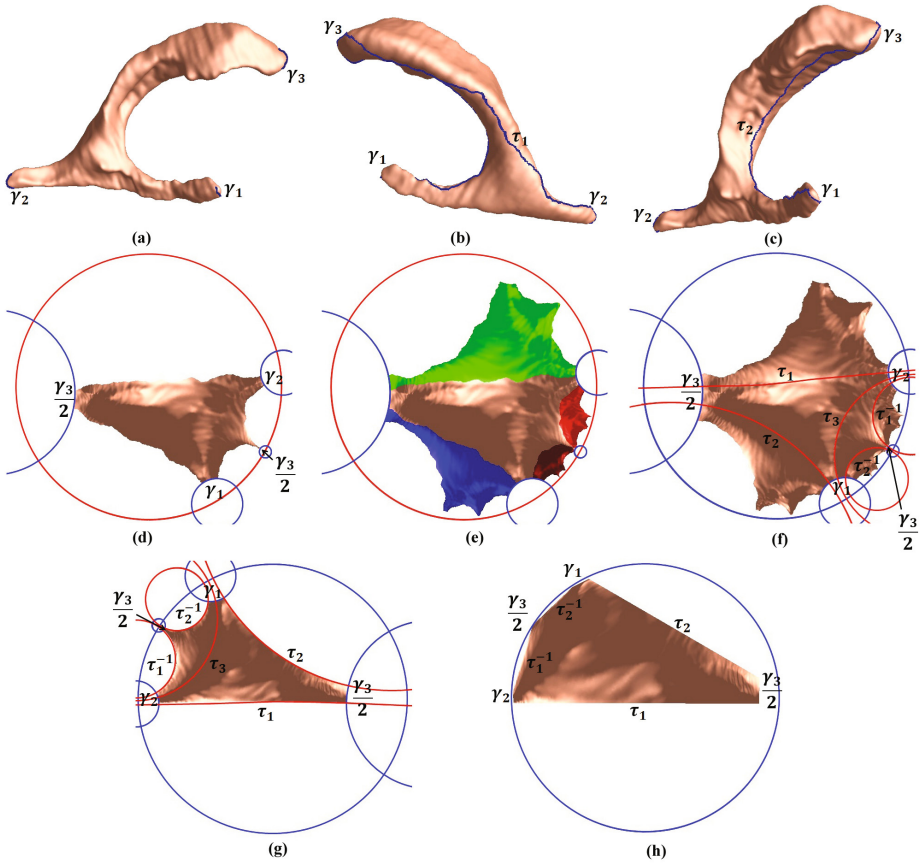


**Fig. 3.** Illustration of hyperbolic conformal parameterization of a left lateral ventricular surface with Ricci flow method.

the lengths of each boundary under the Poincaré disk metric are valid metrics for studying lateral ventricular surface morphology.

In our experiments [40, 49], we compared ventricular surface models extracted from 3D brain MRI scans of 11 individuals with HIV/AIDS and 8 control subjects [7, 8]. We automatically performed topology optimization on each ventricular surface and computed their lengths in the Poincaré disk by the Ricci flow method. For each pair of ventricular surfaces, we obtained a $6 \times 1$ vector, $t = (t_1, t_2, ...t_6)$, which consists of 3 boundary lengths for the left ventricular surface and 3 boundary lengths for right ventricular surface. Given this Teichmüller space coordinate based feature vector, we applied a nearest neighbor classifier based on the Mahalanobis distance, which is

$$d(t) = \sqrt{(t-\mu_{T_c})^T \Sigma_{T_c}^{-1} (t-\mu_{T_c})} + \sqrt{(t-\mu_{T_a})^T \Sigma_{T_a}^{-1} (t-\mu_{T_a})} \qquad (5)$$

where $\mu_{T_c}$, $\mu_{T_a}$, $\Sigma_{T_c}$ and $\Sigma_{T_a}$ are the feature vector mean and covariance for the two groups, respectively. We classified $t$ based on the sign of the distance of $d(t)$, i.e., the subject that is closer to one group mean is classified into that group. For this data set, we performed a leave-one-out test. Our classifier successfully classified all 19 subjects to the correct group and achieved a 100% accuracy rate.

For comparison, we also tested a nearest neighbor classifier associated with a volume feature vector. For each pair of ventricular surface, we measured their volumes, $v = (v_l, v_r)$. We also used nearest neighbor classifier based on the Mahalanobis distance, which is

$$d(v) = \sqrt{(v - \mu_{V_c})^T \Sigma_{V_c}^{-1} (t - \mu_{V_c})} + \sqrt{(t - \mu_{V_a})^T \Sigma_{V_a}^{-1} (t - \mu_{V_a})} \tag{6}$$

where $\mu_{V_c}$, $\mu_{V_a}$, $\Sigma_{V_c}$ and $\Sigma_{V_a}$ are the feature vector mean and covariance for the two groups, respectively. We classified $v$ based on the sign of the distance of $d(v)$, i. e., the subject that is closer to one group mean is classified into that group. In the data set, we performed a leave-one-out test. The classifier based on the simple volume measurement successfully classified only 13 out of 19 subjects to the correct group and achieved a 68.42% accuracy rate.

Studies of ventricular morphology have also used 3D statistical maps to correlate anatomy with clinical measures, but automated ventricular analysis is still difficult because of their highly irregular branching surface shape. The new Teichmüller space shape descriptor requires more validation on other data sets, these experimental results suggest that (1) ventricular surface morphology is altered in HIV/AIDS; (2) volume measures are not sufficient to distinguish HIV patients from controls; and (3) our Teichmüller space feature vector can be used to classify control and patient subjects. Our ongoing work is studying the correlation between the proposed feature vector and clinical measures (e.g., future decline) in an Alzheimer's Disease dataset.

### 4.2 Registering Lateral Ventricular Surfaces via the Klein Model

Here we report our preliminary study of applying the proposed method for registering lateral ventricular surfaces. Experiments on a pair of lateral ventricular surfaces from two diagnostic groups showed that our method is promising for registration of high-genus surfaces.

Fig. 4 (a) and (d) are the left ventricular surfaces from a healthy control subject and an HIV/AIDS patient, respectively. The boundaries were automatically cut by the topology optimization operation introduced in Sec 4.1. By visual observation, it is obvious that the volume of the lateral ventricular surface of the HIV/AIDS patient is larger than that of the control subject. This characteristic is also represented by the corresponding Poincaré models and Klein models. Furthermore, despite of the shape difference, the Klein disks of the two surface are quite similar, which provides a promising initial condition for further registration with constrained harmonic map [8] or surface fluid registration [56]. One of the most advantageous properties of our method over the method in [8] is that surface conformal parameterization with the new method has no singularities.

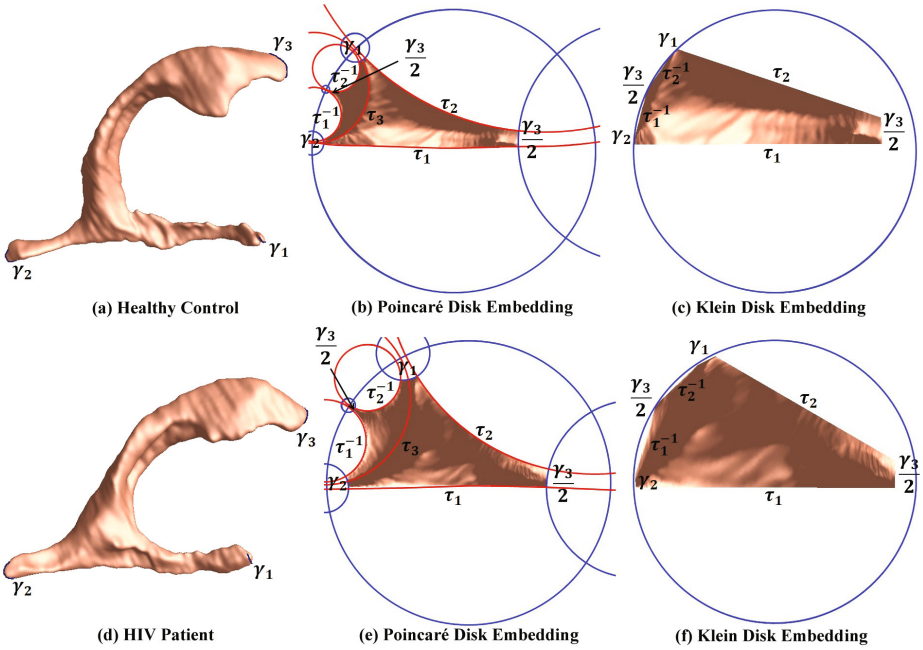


**Fig. 4.** Comparison of two different lateral ventricular surfaces and their hyperbolic parameterizations. The Klein model parameterization provides an intrinsic and stable domain for registration.

All surface information may be used for registration. Intuitively, more usable parameter space in the canonical space is better to match subtle surface features. In our future work, we will apply the proposed pipeline to register high-genus surfaces in big imaging dataset and compare our experimental results with prior methods [8].

## 5 Discussion and Future Work

In this paper, we propose a stable way to compute hyperbolic conformal parameterization for surfaces with complicated topology structure. Given a topological pant surface, for example, the discrete Ricci flow can be applied to embed it into a Poincaré disk. Its Teichmüller space coordinate is calculated from the lengths of its three boundaries under hyperbolic metric. Further, we may transform the Poincaré disk model to Klein model, where a convex polygon is suitable to generate diffeomorphisms between high genus surfaces. We demonstrated our work in lateral ventricle surfaces for HIV/AIDS research.

Our algorithm is based on solving elliptic partial differential equations, so the computation is stable. The computation is also insensitive to the surface triangular mesh quality so it is robust to the digitization errors in the 3D surface reconstruction. Overall, it provides an intrinsic and stable way to compute

surface conformal structure based shape index for further morphometry study. Although our current work focuses on topological pant surfaces, for surfaces with more complicated topologies, their Teichmüller coordinates and Klein model parameterizations can still be computed using the hyperbolic metric. If the surface has Euler number $\chi$, $\chi < 0$, the surface can be decomposed to $-\chi$ number of pants, where the cutting curves are also geodesics under the hyperbolic metric. Furthermore, two pants sharing a common cutting curve can be glued together with a specific twisting angle and it can also be converted to the polygon under the Klein model. The lengths of all cutting geodesics and the twisting angles associated with them form the Teichmüller coordinates of the surface. In the future, we will further explore and validate numerous applications of the hyperbolic Ricci flow method in neuroimaging and shape analysis research.

## References


1. Chung, M.K., Dalton, K.M., Davidson, R.J.: Tensor-based cortical surface morphometry via weighted spherical harmonic representation. IEEE Trans. Med. Imaging 27(8), 1143–1151 (2008)
2. Styner, M., Lieberman, J.A., McClure, R.K., Weinberger, D.R., Jones, D.W., Gerig, G.: Morphometric analysis of lateral ventricles in schizophrenia and healthy controls regarding genetic and disease-specific factors. Proc. Natl. Acad. Sci. U. S. A. 102(13), 4872–4877 (2005)
3. Pizer, S.M., Fritsch, D.S., Yushkevich, P.A., Johnson, V.E., Chaney, E.L.: Segmentation, registration, and measurement of shape variation via image object shape. IEEE Trans. Med. Imaging 18(10), 851–865 (1999)
4. Davies, R.H., Twining, C.J., Allen, P.D., Cootes, T.F., Taylor, C.J.: Shape discrimination in the hippocampus using an MDL model. Inf. Process Med. Imaging 18, 38–50 (2003)
5. Miller, M.I., Trouve, A., Younes, L.: On the metrics and euler-lagrange equations of computational anatomy. Annu. Rev. Biomed. Eng. 4, 375–405 (2002)
6. Thompson, P.M., Toga, A.W.: A framework for computational anatomy. Computing and Visualization in Science 5, 1–12 (2002)
7. Thompson, P.M., Dutton, R.A., Hayashi, K.M., Lu, A., Lee, S.E., Lee, J.Y., Lopez, O.L., Aizenstein, H.J., Toga, A.W., Becker, J.T.: 3D mapping of ventricular and corpus callosum abnormalities in HIV/AIDS. NeuroImage 31(1), 12–23 (2006)
8. Wang, Y., Zhang, J., Gutman, B., Chan, T.F., Becker, J.T., Aizenstein, H.J., Lopez, O.L., Tamburo, R.J., Toga, A.W., Thompson, P.M.: Multivariate tensor-based morphometry on surfaces: Application to mapping ventricular abnormalities in HIV/AIDS. NeuroImage 49(3), 2141–2157 (2010)
9. Ashburner, J., Friston, K.: Multimodal image coregistration and partitioning–a unified framework. Neuroimage 6(3), 209–217 (1997)
10. Christensen, G.E., Rabbitt, R.D., Miller, M.I.: Deformable templates using large deformation kinematics. IEEE Trans. Image Process 5(10), 1435–1447 (1996)
11. Shen, D., Davatzikos, C.: HAMMER: hierarchical attribute matching mechanism for elastic registration. IEEE Trans. Med. Imaging 21(11), 1421–1439 (2002)
12. Fischl, B., Sereno, M.I., Dale, A.M.: Cortical surface-based analysis II: Inflation, flattening, and a surface-based coordinate system. NeuroImage 9(2), 195–207 (1999)

13. Thompson, P.M., Hayashi, K.M., Sowell, E.R., Gogtay, N., Giedd, J.N., Rapoport, J.L., de Zubicaray, G.I., Janke, A.L., Rose, S.E., Semple, J., Doddrell, D.M., Wang, Y., van Erp, T.G.M., Cannon, T.D., Toga, A.W.: Mapping cortical change in Alzheimer's disease, brain development, and schizophrenia. NeuroImage 23(suppl. 1), S2–S18 (2004)
14. Thompson, P.M., Toga, A.W.: A surface-based technique for warping 3-dimensional images of the brain. IEEE Trans. Med. Imag. 15(4), 1–16 (1996)
15. Van Essen, D.C., Drury, H.A., Dickson, J., Harwell, J., Hanlon, D., Anderson, C.H.: An integrated software suite for surface-based analyses of cerebral cortex. J. Am. Med. Inform. Assoc. 8(5), 443–459 (2001)
16. Bakircioglu, M., Joshi, S., Miller, M.I.: Landmark matching on brain surfaces via large deformation diffeomorphisms on the sphere. In: Proc. SPIE Medical Imaging, vol. 3661, pp. 710–715 (1999)
17. Leow, A., Yu, C.L., Lee, S.J., Huang, S.C., Nicolson, R., Hayashi, K.M., Protas, H., Toga, A.W., Thompson, P.M.: Brain structural mapping using a novel hybrid implicit/explicit framework based on the level-set method. NeuroImage 24(3), 910–927 (2005)
18. Yeo, B.T., Sabuncu, M.R., Vercauteren, T., Ayache, N., Fischl, B., Golland, P.: Spherical demons: fast diffeomorphic landmark-free surface registration. IEEE Trans. Med. Imaging 29(3), 650–668 (2010)
19. Davatzikos, C., Vaillant, M., Resnick, S.M., Prince, J.L., Letovsky, S., Bryan, R.N.: A computerized approach for morphological analysis of the corpus callosum. J. Comput. Assist. Tomogr. 20(1), 88–97 (1996)
20. Auzias, G., Colliot, O., Glaunes, J.A., Perrot, M., Mangin, J.F., Trouve, A., Baillet, S.: Diffeomorphic brain registration under exhaustive sulcal constraints. IEEE Trans. Med. Imaging 30(6), 1214–1227 (2011)
21. Bookstein, F.L.: Shape and the information in medical images: a decade of the morphometric synthesis. In: Mathematical Methods in Biomedical Image Analysis, Proceedings of the Workshop, pp. 2–12 (June 1996)
22. Joshi, S.H., Cabeen, R.P., Joshi, A.A., Sun, B., Dinov, I., Narr, K.L., Toga, A.W., Woods, R.P.: Diffeomorphic sulcal shape analysis on the cortex. IEEE Trans. Med. Imaging 31(6), 1195–1212 (2012)
23. Pantazis, D., Joshi, A., Jiang, J., Shattuck, D.W., Bernstein, L.E., Damasio, H., Leahy, R.M.: Comparison of landmark-based and automatic methods for cortical surface registration. Neuroimage 49(3), 2479–2493 (2010)
24. Zhong, J., Phua, D.Y., Qiu, A.: Quantitative evaluation of LDDMM, FreeSurfer, and CARET for cortical surface mapping. Neuroimage 52(1), 131–141 (2010)
25. Joshi, S.C., Miller, M.I., Grenander, U.: On the geometry and shape of brain submanifolds. IEEE Trans. Patt. Anal. Mach. Intell. 11, 1317–1343 (1997)
26. Durrleman, S., Pennec, X., Trouve, A., Thompson, P.M., Ayache, N.: Inferring brain variability from diffeomorphic deformations of currents: An integrative approach. Medical Image Analysis 12(5), 626–637 (2008)
27. Vaillant, M., Qiu, A., Glaunes, J., Miller, M.I.: Diffeomorphic metric surface mapping in subregion of the superior temporal gyrus. Neuroimage 34(3), 1149–1159 (2007)
28. Trouvé, A., Younes, L.: Metamorphoses through Lie group action. Found. Comp. Math., 173–198 (2005)
29. Boyer, D.M., Lipman, Y., St Clair, E., Puente, J., Patel, B.A., Funkhouser, T., Jernvall, J., Daubechies, I.: Algorithms to automatically quantify the geometric similarity of anatomical surfaces. Proc. Natl. Acad. Sci. U.S.A. 108, 18221–18226 (2011)

30. Fischl, B., Sereno, M.I., Tootell, R.B., Dale, A.M.: High-resolution intersubject averaging and a coordinate system for the cortical surface. Hum. Brain Mapp. 8(4), 272–284 (1999)
31. Pitiot, A., Delingette, H., Toga, A.W., Thompson, P.M.: Learning object correspondences with the observed transport shape measure. Inf. Process. Med. Imaging 18, 25–37 (2003)
32. Wang, Y., Chiang, M.C., Thompson, P.M.: Mutual information-based 3D surface matching with applications to face recognition and brain mapping. In: Proc. of the Tenth IEEE International Conference on Computer Vision, ICCV 2005, vol. 1, pp. 527–534 (October 2005)
33. Younes, L.: Shapes and Diffeomorphisms. Springer (2010)
34. Fletcher, P.T., Lu, C., Pizer, S.M., Joshi, S.: Principal geodesic analysis for the study of nonlinear statistics of shape. IEEE Trans. Med. Imaging 23(8), 995–1005 (2004)
35. Miller, M.I., Qiu, A.: The emerging discipline of Computational Functional Anatomy. Neuroimage 45(suppl. 1), 16–39 (2009)
36. Ashburner, J., Hutton, C., Frackowiak, R., Johnsrude, I., Price, C., Friston, K.: Identifying global anatomical differences: deformation-based morphometry. Hum. Brain Mapp. 6(5-6), 348–357 (1998)
37. Wang, L., Swank, J.S., Glick, I.E., Gado, M.H., Miller, M.I., Morris, J.C., Csernansky, J.G.: Changes in hippocampal volume and shape across time distinguish dementia of the Alzheimer type from healthy aging. Neuroimage 20(2), 667–682 (2003)
38. Davatzikos, C.: Spatial normalization of 3D brain images using deformable models. J. Comput. Assist. Tomogr. 20(4), 656–665 (1996)
39. Jin, M., Zeng, W., Luo, F., Gu, X.: Computing Teichmüller shape space. IEEE Trans. Vis. Comput. Graphics 15(3), 504–517 (2009)
40. Wang, Y., Dai, W., Gu, X., Chan, T.F., Yau, S.-T., Toga, A.W., Thompson, P.M.: Teichmüller Shape Space Theory and Its Application to Brain Morphometry. In: Yang, G.-Z., Hawkes, D., Rueckert, D., Noble, A., Taylor, C. (eds.) MICCAI 2009, Part II. LNCS, vol. 5762, pp. 133–140. Springer, Heidelberg (2009)
41. Shi, Y., Lai, R., Gill, R., Pelletier, D., Mohr, D., Sicotte, N., Toga, A.W.: Conformal Metric Optimization on Surface (CMOS) for Deformation and Mapping in Laplace-Beltrami Embedding Space. In: Fichtinger, G., Martel, A., Peters, T. (eds.) MICCAI 2011, Part II. LNCS, vol. 6892, pp. 327–334. Springer, Heidelberg (2011)
42. Kurtek, S., Klassen, E., Ding, Z., Jacobson, S.W., Jacobson, J.L., Avison, M.J., Srivastava, A.: Parameterization-invariant shape comparisons of anatomical surfaces. IEEE Trans. Med. Imaging 30(3), 849–858 (2011)
43. Hurdal, M.K., Stephenson, K.: Cortical cartography using the discrete conformal approach of circle packings. NeuroImage 23, S119–S128 (2004)
44. Angenent, S., Haker, S., Tannenbaum, A.R., Kikinis, R.: Conformal Geometry and Brain Flattening. In: Taylor, C., Colchester, A. (eds.) MICCAI 1999. LNCS, vol. 1679, pp. 271–278. Springer, Heidelberg (1999)
45. Ju, L., Hurdal, M.K., Stern, J., Rehm, K., Schaper, K., Rottenberg, D.: Quantitative evaluation of three surface flattening methods. NeuroImage 28(4), 869–880 (2005)
46. Tosun, D., Prince, J.: A geometry-driven optical flow warping for spatial normalization of cortical surfaces. IEEE Trans. Med. Imag. 27(12), 1739–1753 (2008)

47. Gu, X., Wang, Y., Chan, T.F., Thompson, P.M., Yau, S.T.: Genus zero surface conformal mapping and its application to brain surface mapping. IEEE Trans. Med. Imag. 23(8), 949–958 (2004)
48. Wang, Y., Lui, L.M., Gu, X., Hayashi, K.M., Chan, T.F., Toga, A.W., Thompson, P.M., Yau, S.T.: Brain surface conformal parameterization using Riemann surface structure. IEEE Trans. Med. Imag. 26(6), 853–865 (2007)
49. Wang, Y., Dai, W., Gu, X., Chan, T.F., Toga, A.W., Thompson, P.M.: Studying brain morphology using Teichmüller space theory. In: IEEE 12th International Conference on Computer Vision, ICCV 2009, pp. 2365–2372 (September 2009)
50. Wang, Y., Shi, J., Yin, X., Gu, X., Chan, T.F., Yau, S.T., Toga, A.W., Thompson, P.M.: Brain surface conformal parameterization with the Ricci flow. IEEE Trans. Med. Imaging 31(2), 251–264 (2012)
51. Wang, Y., Gu, X., Chan, T.F., Thompson, P.M., Yau, S.T.: Conformal Slit Mapping and Its Applications to Brain Surface Parameterization. In: Metaxas, D., Axel, L., Fichtinger, G., Székely, G. (eds.) MICCAI 2008, Part I. LNCS, vol. 5241, pp. 585–593. Springer, Heidelberg (2008)
52. Zeng, W., Samaras, D., Gu, X.: Ricci flow for 3D shape analysis. IEEE Trans. Patt. Anal. Mach. Intell. 32, 662–677 (2010)
53. Gu, X., Yau, S.T.: Computational Conformal Geometry. International Press (2008)
54. Wikipedia: Hyperbolic geometry — Wikipedia, the free encyclopedia (2012)
55. Luo, F., Gu, X., Dai, J.: Variational Principles for Discrete Surfaces. International Press (2008)
56. Shi, J., Thompson, P.M., Gutman, B., Wang, Y.: Surface fluid registration of conformal representation: application to detect disease effect and genetic influence on hippocampus. Submitted to NeuroImage (2012)
57. Carmichael, O.T., Thompson, P.M., Dutton, R.A., Lu, A., Lee, S.E., Lee, J.Y., Kuller, L.H., Lopez, O.L., Aizenstein, H.J., Meltzer, C.C., Liu, Y., Toga, A.W., Becker, J.T.: Mapping ventricular changes related to dementia and mild cognitive impairment in a large community-based cohort. In: 3rd IEEE International Symposium on Biomedical Imaging: Nano to Macro, pp. 315–318 (April 2006)
58. Ferrarini, L., Palm, W.M., Olofsen, H., van Buchem, M.A., Reiber, J.H., Admiraal-Behloul, F.: Shape differences of the brain ventricles in Alzheimer's disease. NeuroImage 32(3), 1060–1069 (2006)
59. Chou, Y., Leporé, N., de Zubicaray, G.I., Carmichael, O.T., Becker, J.T., Toga, A.W., Thompson, P.M.: Automated ventricular mapping with multi-atlas fluid image alignment reveals genetic effects in Alzheimer's disease. NeuroImage 40(2), 615–630 (2008)